科学通报 2025 年 第 70 卷 第 6 期: 655 ~ 664
高性能铅锡硫族热电材料专辑 进 展
《中国科学》杂志社 SCIENCE CHINA PRESS

n型硒化锡晶体热电材料研究进展

宿力中*, 冯孝坤

太原科技大学材料科学与工程学院, 太原 030024

* 联系人, E-mail: sulizhong@tyust.edu.cn

2024-07-22 收稿, 2024-08-20 修回, 2024-08-22 接受, 2024-08-23 网络版发表

太原科技大学引进人才科研启动基金(20232094)和山西省优秀来晋博士科研资助项目(20242010)资助

摘要 构建高性能热电器件需要拥有性能相匹配的高性能p型与n型热电材料. 硒化锡(SnSe)晶体因其优异的热电性能引起了热电领域的广泛关注. 当前, p型SnSe晶体在300~773 K可取得~2.2的平均无量纲热电优值(ZT_{ave}), 300 K时ZT可达~1.5; n型SnSe晶体在300~773 K也可获得1.7的ZT_{ave}, 但300 K时ZT仅为~0.5, 与p型SnSe晶体仍有不小差距. 优化n型SnSe晶体的热电性能成为了实现全SnSe基热电器件的研究重点. 本文总结了n型SnSe晶体的研究进展, 分析了不同施主杂质掺杂的n型SnSe晶体热电输运特性的异同, 围绕载流子散射因子对比了固溶硒化铅对n型SnSe晶体面内与面外电输运性能造成的不同影响, 介绍了SnSe相变对其热导率的影响, 对n型SnSe晶体热电材料后续研究的重点与难点进行了展望.

关键词 热电材料, 晶体, 层状结构, 相变材料, n型硒化锡

热电能源转换技术是一种能够依托塞贝克效应(Seebeck effect)和帕尔贴效应(Peltier effect)实现电能与热能直接相互转换的技术, 即能够实现温差发电与通电制冷(制热), 具有体积小、无机械振动、无噪音、绿色环保等特点[1,2]. 实现高效热电能源转换技术的基础是开发高性能热电材料. 热电材料的性能主要由无量纲热电优值ZT决定: $ZT = [\sigma S^2/(\kappa_{lat} + \kappa_{ele})]T$, 其中$\sigma$、$S$、$\kappa_{lat}$、$\kappa_{ele}$、$T$分别为电导率、塞贝克系数、晶格热导率、电子热导率以及热力学温度, σS^2又被称为功率因子(power factor, PF), κ_{lat}与κ_{ele}之和为总热导率κ_{tot}, ZT越大, 材料热电性能越好[3,4]. 经过长期发展, 研究人员利用调制掺杂[5,6]、能带结构调整[7~9]、晶体结构调控[10~12]、多尺寸缺陷设计[13~15]、复合材料设计[16~18]、开发本征低热导率材料[19~21]等方法解耦决定ZT的各参数之间的耦合关系, 激发出一系列传统热电材料的性能潜力, 也开发出了一系列具有优异热电性能的新材料.

硒化锡(SnSe)是一种具有本征低热导率的宽带隙(~0.86 eV)层状各向异性材料[22]. 2014年, Zhao等人[23]首次报道了本征p型的SnSe晶体的热电性能, 由于其强非谐振性带来的低热导率与面内高载流子迁移率, 在923 K实现了~2.6的最大ZT(ZT_{max}), 引起了热电领域的广泛关注. 经过不断的发展, 目前p型与n型SnSe晶体展现出了非常优异的热电性能, 在300~773 K的平均ZT(ZT_{ave})分别可达~2.2与1.7, 被视为有可能超越碲化铋(Bi_2Te_3)的下一代商用热电材料之一[24~26]. SnSe独特的各向异性晶体结构与相变过程对其性能有十分重要的影响, 室温下, 本征SnSe具有正交的*Pnma*晶体结构, 600~800 K由低对称*Pnma*相持续性相变为高对称*Pnma*相, 最终在~800 K附近由临界相变转变为高温高对称*Cmcm*相[27,28]. SnSe独特的晶体结构赋予了其复杂的能带结构, SnSe价带底附近有4个能量差(~0.15 eV)相近的价带, 导带底附近则有两个能量差约为~0.1 eV的导带, 这一能带结构特点使得SnSe能较容易地实现多能

引用格式: 宿力中, 冯孝坤. n型硒化锡晶体热电材料研究进展. 科学通报, 2025, 70: 655–664
Su L Z, Feng X K. Recent progress in n-type SnSe crystals thermoelectric materials (in Chinese). Chin Sci Bull, 2025, 70: 655–664, doi: 10.1360/TB-2024-0796

© 2024《中国科学》杂志社

带输运. 此外, SnSe随温度演进的相结构变化伴随着其能带结构在动量空间与能量空间的多方位演化, 对其实现优异电输运性能有关键作用[25,29]. 对于价带, 随着温度与晶体结构对称性的提升, SnSe位于布里渊区同一方向的第一价带与第二价带逐渐合并, 形成动量空间的对齐优化了载流子迁移率μ; 第一价带与第三价带之间的能量差逐步减小, 发生能带简并增大了态密度有效质量m^*. SnSe的导带随温度与晶体结构对称性的演化较为简单, 第一导带与第二导带先简并后退简并, 先后优化了n型SnSe的m^*与高温μ. 除温度诱导SnSe相结构变化外, 异质元素的引入也能通过改变原有晶格应力分布而引起SnSe晶体结构对称性的变化, 由此衍生出来的晶体结构对称性优化策略能有效优化p型与n型SnSe晶体的热电性能[30,31]. SnSe的结构特点使p型与n型SnSe表现出不同的电荷密度分布[26,32]. 如图1(b)所示, 不同于p型SnSe较低的层间电荷密度, n型SnSe形成了层间交叠的电荷密度, 这一特点使得n型SnSe具有了“二维声子-三维电荷”的热电输运特性, 沿SnSe的面外方向(晶体学a轴方向)实现了优异的热电性能[32].

铋(Bi)掺杂SnSe晶体(SnSe-Bi)是首个报道的n型SnSe晶体, 但其没有表现出“二维声子-三维电荷”的热电输运特性, 这可能是因为Bi在Sn位的重掺杂破坏了SnSe原有的能带结构. 尽管如此, SnSe-Bi依靠其高温较高的载流子浓度n及超低的κ_{lat}在面内方向(晶体学bc平面方向)实现了~2.2的ZT_{max}, 如图1(c)所示. 然而, SnSe-Bi在室温下的n很低(~10^{16} cm^{-3}), Bi掺杂没有改变n型SnSe的半导体电输运特点[33]. 溴(Br)元素拥有远高于Bi的掺杂效率, Br掺杂SnSe晶体(SnSe-Br)大幅提高了n型SnSe晶体的n, 室温下其n可达1.2 × 10^{19} cm^{-3}[29]. 同时, SnSe-Br通过“二维声子-三维电荷”热电输运特性在面外方向实现了~2.8的ZT_{max}(773 K). 除Br掺杂外, 氯(Cl)、碘(I)掺杂的n型SnSe晶体(SnSe-Cl、SnSe-I)同样具有“二维声子-三维电荷”热电输运特性[26,34], 导致卤素掺杂的n型SnSe晶体在面外方向拥有远高于面内方向的热电性能. Br掺杂PbSe固溶(8%)的n型SnSe晶体(SnSe-Br-8% PbSe)面内方向的高温热电性能远低于SnSe-Bi, 这可能是两者差异巨大的高温n导致的[35]. 当前, 固溶硒化铅(PbSe)是提升卤素掺杂n型SnSe晶体热电性能的主要手

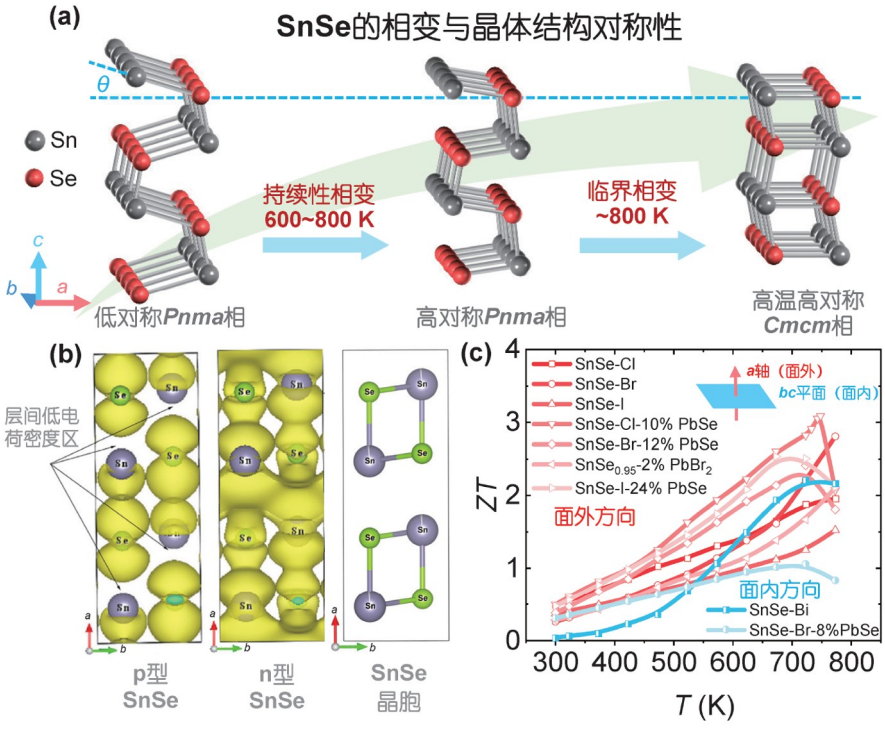


图 1 (网络版彩色)SnSe的结构特点及n型SnSe晶体热电性能. (a) 晶体结构与相变; (b) 电荷密度分布[32], Copyright © 2015, Elsevier B.V.; (c) 几种n型SnSe晶体的ZT值[26,29,31,33,34,36]

Figure 1 (Color online) Structural features and thermoelectric performance of n-type SnSe crystals. (a) The crystal structure and phase transition; (b) the distribution of charge density[32], Copyright © 2015, Elsevier B.V.; (c) the ZT value of several n-type SnSe crystals[26,29,31,33,34,36]

段[26,31,34~36]. PbSe固溶的Cl掺杂n型SnSe晶体(SnSe-Cl-10%PbSe)沿其面外方向可在748 K实现~3.1的超高ZT_{max}, 300~773 K的ZT_{ave}为~1.7, 室温下ZT为~0.5, 在同温区n型热电材料中处于领先地位[26].

虽然n型SnSe晶体表现出了不俗的热电性能, 但其宽温域热电性能及近室温热电性能与p型SnSe晶体相比仍有一定差距, 且n型SnSe晶体在集成热电器件方面远落后于p型SnSe晶体. 当前, 通过晶格素化策略优化的p型SnSe晶体在室温下实现了~1.5的超高ZT, 300~773 K的ZT_{ave}达到了~2.2, 其单臂器件在300 K温差下可实现~12.2%的发电效率, 与n型Bi_2Te_3一同搭建的热电器件也实现了室温下~61.2 K的制冷温差, 与商用Bi_2Te_3热电器件相当[25]. 构建高性能热电器件的前提是开发性能相匹配的高性能n型与p型热电材料, 进一步优化n型SnSe晶体的热电性能、开发其热电器件集成工艺成为实现全SnSe基热电器件的关键挑战. 因此, 本文总结了近年来n型SnSe晶体研究领域的工作进展, 比较了不同元素掺杂n型SnSe晶体的热电输运特性, 对比了目前主要的n型SnSe晶体性能优化方式——固溶PbSe对n型SnSe晶体面内与面外方向的载流子散射因子r及电输运性能的影响, 介绍了SnSe的持续性相变与临界相变对其热导率的影响, 讨论了n型SnSe晶体未来发展的主要挑战与困难.

1 n型硒化锡晶体的电输运性能

虽然理论计算结果表明n型SnSe晶体面外方向的热电性能应高于面内方向, 但首个报道的n型SnSe晶体SnSe-Bi却在面内方向实现了~2.2的ZT_{max}, 远高于面外的~0.8[32,33]. 除此之外, SnSe-Bi与卤素掺杂n型SnSe晶体的n也有很大不同, SnSe-Bi的载流子浓度随温度呈现不断上升的趋势, 室温下的n仅为10^{16} cm^{-3}左右, 773 K时可达~2.1 × 10^{19} cm^{-3}; 不同于SnSe-Bi, 卤素掺杂的n型SnSe晶体室温下具有较高的n, SnSe-I能达到的最高n为~5.6×10^{18} cm^{-3}, SnSe-Br为~1.2×10^{19} cm^{-3}, SnSe-Cl为~8.6×10^{18} cm^{-3}, 这一结果与理论计算得到的I_{Se}^-缺陷远高于Cl_{Se}^-和Br_{Se}^-缺陷的形成能的结果一致[34,37,38]; 随着温度的升高, 卤素掺杂的n型SnSe晶体的n总体随温度呈下降趋势.

图2给出了不同卤素掺杂的n型SnSe晶体面外方向电输运性能. 过低的n使SnSe-I的σ为三者之中的最低; 虽然SnSe-Cl的n也低于SnSe-Br, 但SnSe-Cl与SnSe-Br表现出几乎完全一致的σ. 三种卤素元素掺杂的n型SnSe晶体的S的大小关系与其n的大小关系保持一致. 整体来看, SnSe-Cl几乎在整个温区内都保持着电输运性能的优势; SnSe-Br则因其较高的n在高温下获得了更大的PF; 相较于SnSe-Br, SnSe-I虽然在300~423 K的范围内拥有更高的PF, 但过低的n使其中高温电输运性能远低于SnSe-Cl/Br, 如图2(b)所示. 除掺杂效率不同导致的n不同外, 不同卤素掺杂n型SnSe的电输运性能差异主要由m^*与形变势Ξ的不同引起. 利用声学声子散射假设($r = -0.5$)的单抛物带模型计算得到的m^*如图2(c)所示, SnSe-Cl/Br几乎具有相同的m^*, SnSe-I的m^*则略低于SnSe-Cl/Br; SnSe-I较低的m^*使其保持了较高的μ, SnSe-Cl则因其较低的Ξ获得了SnSe-Cl/Br/I中最高的μ; SnSe-Br与SnSe-I的Ξ大致相同, 但较高的m^*使其μ为三者之中的最低, 如图2(d)所示. 实际上, 利用声学声子散射假设计算得到的卤素掺杂n型SnSe晶体的m^*的数值是不准确的, 卤素掺杂的n型SnSe晶体在面外方向并不严格遵守声学声子散射($r \neq -0.5$), 但这并不影响计算结果给出的卤素掺杂n型SnSe晶体m^*的相对大小关系.

卤素掺杂的n型SnSe晶体具有明显的S各向异性, 以SnSe-Cl为例, 其面内与面外S的差异随温度的升高不断增大, 如图3(a)所示. 单抛物带模型下S可以表示为: $S = \pm\frac{k_B}{e}\left[\frac{(r+2.5)F_{(r+1.5)}(\eta)}{(r+1.5)F_{(r+0.5)}(\eta)} - \eta\right]$, 其中$k_B$为玻尔兹曼常数, e为电子电荷量, $\eta = E_F / k_BT$为简约费米能级, $F_n(\eta)$为费米积分[34]. 可见, S仅为η与r的函数, 由于能量不具有各向异性, 因此SnSe-Cl的各向异性S表明其具有各向异性的r. 对于特定的载流子散射机制, r具有某一固定值. 当材料中存在对载流子的混合散射且多种散射机制具有不同的r时, 根据马西森定则, 总弛豫时间可表示为: $\frac{1}{\tau} = \frac{1}{\tau_{0,1}E^{r_1}} + \frac{1}{\tau_{0,2}E^{r_2}} + \cdots$, 其中$\tau$为弛豫时间($\tau = \tau_0E^r$), E为能量; 虽然此时已不能对总弛豫时间在整个E区间内使用τ_0E^r的形式表达, 但在E的不同取值范围内([E_1, E_2]), 仍可采用$\tau = \tau_0E^r$的函数表达式对总弛豫时间进行拟合, 即$\frac{1}{\tau} = \frac{1}{\tau_{0,1}E^{r_1}} + \frac{1}{\tau_{0,2}E^{r_2}} \approx \frac{1}{\tau_0E^r}$, 这意味着材料的$r$不再为定值, 其值随能量范围的变化而变化. r对S有着十分显著的影响, 以简并条件为例, 此时S可近似表达为$S = \frac{8\pi^2k_B^2}{3eh^2}m^*T\left(\frac{\pi}{3n}\right)^{\frac{2}{3}}(r+1.5)$, 当$r$由−0.5增大至−0.3时, S将提升20%. 对于仅存在声学支声子散射的材料,

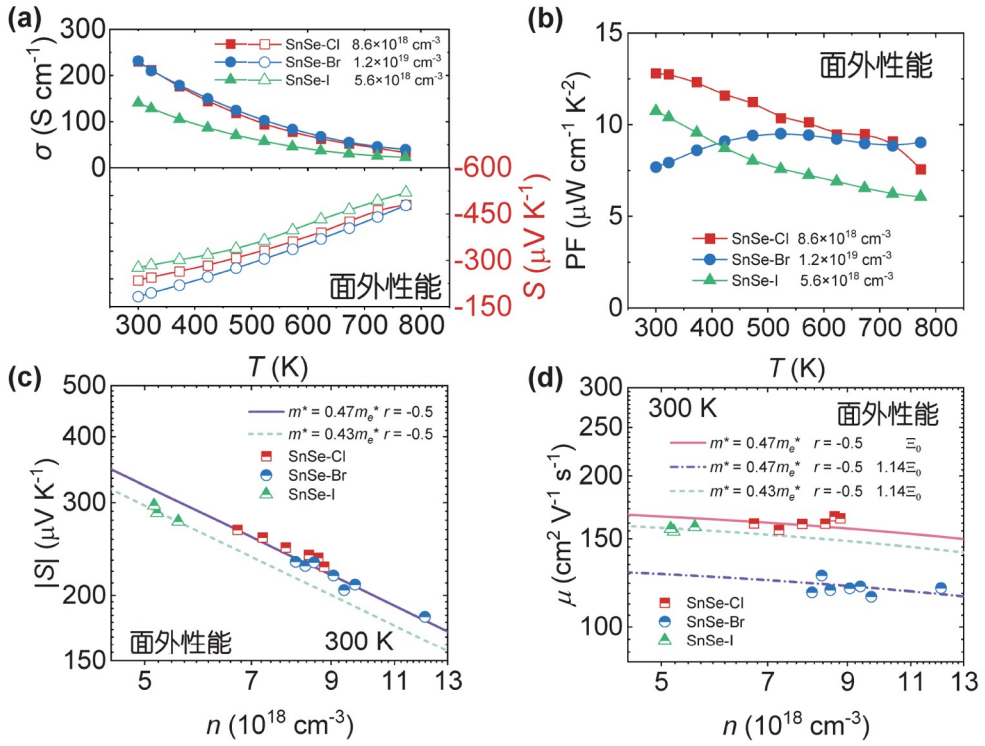


图 2 (网络版彩色)卤素掺杂的n型SnSe晶体电输运性能对比[26,29,34]. (a) 电导率σ与塞贝克系数S; (b) 功率因子PF; (c) 300 K下塞贝克系数的绝对值$|S|$与载流子浓度n的关系; (d) 300 K下载流子迁移率μ与n的关系

Figure 2 (Color online) Comparison of the electrical transport properties of halogen-doped n-type SnSe crystals[26,29,34]. (a) Electrical conductivity σ versus Seebeck coefficient S; (b) power factor PF; (c) absolute value of the Seebeck coefficient $|S|$ as a function of carrier concentration n at 300 K; (d) carrier mobility μ as a function of n at 300 K

当在其中引入其他散射机制形成准声子散射时, μ与T的关系可近似表示为$\mu \propto T^{-1+r}$. 卤素掺杂的n型SnSe晶体符合准声子散射条件[34]. SnSe-Cl的各向异性r会导致其面内与面外的σ与μ随T变化的趋势不同, 而其面内与面外的r也可由两方向μ随T的变化近似求出, 如图3(b)所示. SnSe-Cl面内方向较符合声学声子散射(r = −0.48), 面外方向的r(−0.31)则明显大于面内方向. 考虑面内与面外r的差异后, 利用单抛物带模型计算得到的两方向m^*取得了良好的一致性, 且与理论计算得到的SnSe第一导带底的有效质量m^*_{CBM1}一致, 室温下约为~0.42 m_e; 523 K后m^*大于m^*_{CBM1}, 表明SnSe-Cl的导带发生简并并实现双导带输运, m^*约为0.5 m_e[26,29]. 实际上, 面外拥有更大r是SnSe-Cl/Br/I的共同特点. 图3(d)给出了考虑r后SnSe-Cl/Br/I在300 K时的m^*, 其相对大小关系与前文分析一致.

SnSe独特的晶体结构与相变过程使其能够通过调控晶体结构对称性实现热电性能的优化. 相比于SnSe-Br/I, SnSe-Cl具有更低Ξ的原因就在于Cl掺杂使SnSe具有更高的晶体结构对称性, 如图4(a)所示[26]. 固溶PbSe之所以能成为当前n型SnSe晶体热电性能的主要优化手段, 除化学成分变化引起的优化作用外, 因固溶引入的额外应力对SnSe晶体结构对称性的改变同样对其电输运性能有不可忽视的影响. 固溶PbSe能显著降低SnSe的临界相变温度(*Pnma* → *Cmcm*), 如图4(b)所示[31]. 相变温度的降低意味着固溶PbSe使SnSe能在较低的温度下表现出更高的晶体结构对称性, 其与固溶PbSe引入的额外晶体应力一同导致了PbSe固溶的SnSe晶体对称性的显著提升. 固溶PbSe还能明显改变SnSe的导带结构, 如图4(c)所示[31]. SnSe的第一导带底CBM1与第二导带底CBM2的能量差随着PbSe的引入明显降低, 促进了SnSe导带的简并; 此外, PbSe固溶后CBM1与CBM2能量差的最小值所在温度降低了近300 K, PbSe固溶带来的相变温度降低及晶体结构对称性提高可能是导致这一现象的原因之一. 除促进能带简并优化S外, 固溶PbSe加剧了n型SnSe晶体r的各向异性, 对面内与面外S造成了相反的影响[34,35]. 如图4(d)所

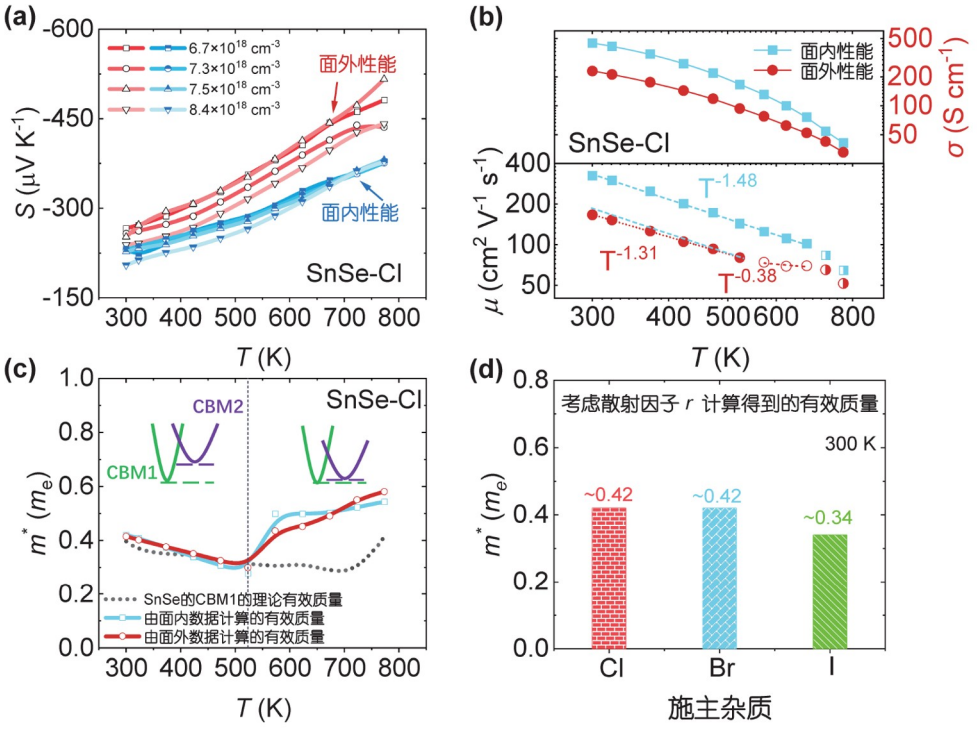


图 3 (网络版彩色)n型SnSe晶体电输运性能的各向异性. (a) 塞贝克系数S; (b) 载流子迁移率μ[34]; (c) 态密度有效质量m^*随温度T的演进[34], Copyright © 2019, Wiley-VCH Verlag GmbH & Co. KGaA, Weinheim; (d) 300 K下不同卤素掺杂n型SnSe晶体的m^*[34,35]

Figure 3 (Color online) Anisotropy of the electrical transport properties of n-type SnSe crystals. (a) Seebeck coefficient S; (b) carrier mobility μ[34]; (c) density of states effective mass m^* as a function of temperature T[34], Copyright © 2019, Wiley-VCH Verlag GmbH & Co. KGaA, Weinheim; (d) m^* of n-type SnSe crystals with different halogen doping at 300 K[34,35]

示，PbSe固溶降低了n型SnSe晶体面内方向的r，导致SnSe-Br-x%PbSe面内方向的S实测值均位于利用SnSe-Br面内性能计算得到的理论线(r = −0.5)之下, 考虑r变化后计算得到SnSe-Br-x%PbSe样品面内方向S模拟值重新回到理论线附近，表明其在300 K下仍为单导带输运；不同于面内方向，PbSe固溶的I掺杂n型SnSe晶体SnSe-I-x%PbSe面外方向的r明显增大，考虑其r变化后发现PbSe固溶含量≥16%时(且$n \geqslant \sim 14.7 \times 10^{18}$ cm^{-3}), I掺杂SnSe晶体在室温下实现双导带输运，固溶PbSe通过能带简并与增大r实现了n型SnSe晶体面外方向电输运性能的显著优化. 对于面内性能，固溶PbSe带来的r降低使优化效果大幅降低.

2 n型硒化锡晶体的热输运性能

SnSe的强非谐振性使其具有较低的本征κ_{lat}，引入施主杂质可进一步降低κ_{lat}. 不同卤素掺杂的n型SnSe的κ_{lat}存在一定差别, 且这一差别与其晶体结构对称性, 即不同杂质掺杂导致的SnSe晶格应力变化的大小密切相关. 如图5(a)所示[26,31,34]，300 K下SnSe-Cl相比于SnSe-Br/I表现出更低的κ_{lat}，SnSe-Br与SnSe-I的κ_{lat}差异较小，SnSe-Cl较低的κ_{lat}与其具有更高晶体结构对称性的结果一致，Cl掺杂在SnSe晶格中引起了更多的应力波动，使其获得了更高的晶体结构对称性；473 K时SnSe-Cl与SnSe-Br/I的κ_{lat}差异减小，这可能是由SnSe-Cl与SnSe-Br随温度降低的晶体结构对称性差异的减小引起；直至723 K，SnSe-Cl与SnSe-I之间κ_{lat}的差异进一步减小，但SnSe-Br的κ_{lat}为三者之中的最低，这可能与SnSe-Br在高温下迅速提升的晶体结构对称性有关. 固溶PbSe能显著降低n型SnSe晶体的κ_{lat}，但其降低κ_{lat}的作用主要体现在中低温区；723 K时，SnSe-I-24%PbSe的κ_{lat}略高于SnSe-I-16%PbSe，这主要是因为固溶24% PbSe后SnSe的临界相变温度大大提前，723 K的SnSe-I-24%PbSe已处于$Cmcm$相. 如图5(b)所示, 固溶PbSe引起的应力波动是其能有效降低SnSe的κ_{lat}的主要原因，这与固溶PbSe后显著提升的晶体结构对称性保持一致[31]. 遗憾的是，目前没有大比例固溶PbSe的Cl/Br掺

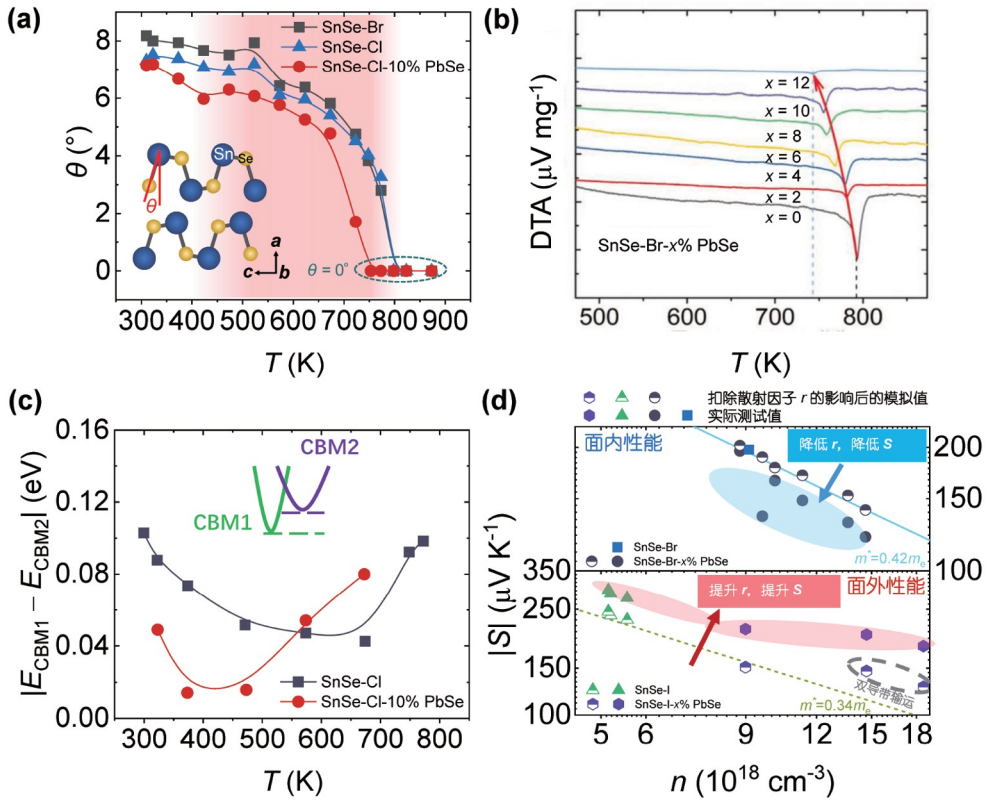


图 4 (网络版彩色)PbSe固溶对n型SnSe晶体的结构与电输运性能的影响. (a) 晶体结构对称性随温度T的演化[26], Copyright © 2022, American Association for the Advancement of Science; (b) 差热分析(DTA)证明临界相变温度的降低[31], Copyright © 2019, Wiley-VCH Verlag GmbH & Co. KGaA, Weinheim; (c) 第一导带底CBM1与第二导带底CBM2的能量差随温度T的演进[31]; (d) 300 K下PbSe固溶对n型SnSe晶体面内与面外的塞贝克系数S的影响[34,35]

Figure 4 (Color online) Effects of PbSe alloying on the structure and electrical transport properties of n-type SnSe crystals. (a) Crystal structure symmetry as a function of temperature T[26], Copyright © 2022, American Association for the Advancement of Science; (b) differential thermal analysis (DTA) demonstrating the decrease of critical phase transition temperatures[31], Copyright © 2019, Wiley-VCH Verlag GmbH & Co. KGaA, Weinheim; (c) energy difference between the lowest conduction band minimum CBM1 and the second lowest conduction band minimum CBM2 as a function of temperature T[31]; (d) PbSe alloying shows different effects on the Seebeck coefficient S of n-type SnSe crystals along the in-plane and out-of-plane directions at 300 K[34,35]

杂SnSe晶体热电性能的报道，大比例固溶PbSe时，其对n型SnSe晶体热电输运特性的影响还有待进一步探究.

SnSe的特殊晶体结构与相变为其带来优异热电性能的同时，也为评估其相变期间的热导率带来了挑战[39,40]. 依据相变速度模型，材料相变期间的热导率可表示为$\kappa_{\rm tot} = D\rho C_{p,0}\left(1+\frac{\Delta H}{C_{p,0}}\frac{{\rm d}t}{{\rm d}T}\frac{{\rm d}a}{{\rm d}t}\right)$，其中$D$为热扩散系数，$\rho$为密度，$C_{p,0}$为运用Dulong-Petit定律计算得到的定压热容，ΔH为相变焓，a为相变终点相的摩尔分数，t为时间[26]. ΔH和da/dt对相变期间材料的热传输起到关键作用. 考虑两个极限条件：(1) 当相变速率很低(da/dt →0)或ΔH很低(ΔH→0)时，材料相变期间$\kappa_{\rm tot} = D\rho C_{p,0}$，即材料相变不影响材料的热输运性能；(2) 当相变速率非常快时(da/dt→∞)，材料相变期间$\kappa_{\rm tot} = D\rho C_{p,{\rm m}}$，其中$C_{p,{\rm m}}$为快速升温速率下实际测量得到的热容. 图6(a)给出了在5 K min^{-1}的升温速率下不同材料的相变速度[26,40,41]，相比于其他相变热电材料，SnSe拥有较低的相变速度，且固溶PbSe能进一步降低其相变速度；材料升温速率能够明显影响其相变速率，考虑到5 K min^{-1}的升温速率远低于使用激光法测量热导率时样品的升温速率，SnSe在热扩散系数测量时具有更低的相变速度. 图6(b)给出了利用相变速度模型修正的SnSe-Cl-10%PbSe样品的$\kappa_{\rm lat}$. SnSe的持续性相变对其热导率没有产生明显影响，这可能是SnSe持续性相变的相变速度过低导致的；SnSe的临界相变对其热导率有显著影

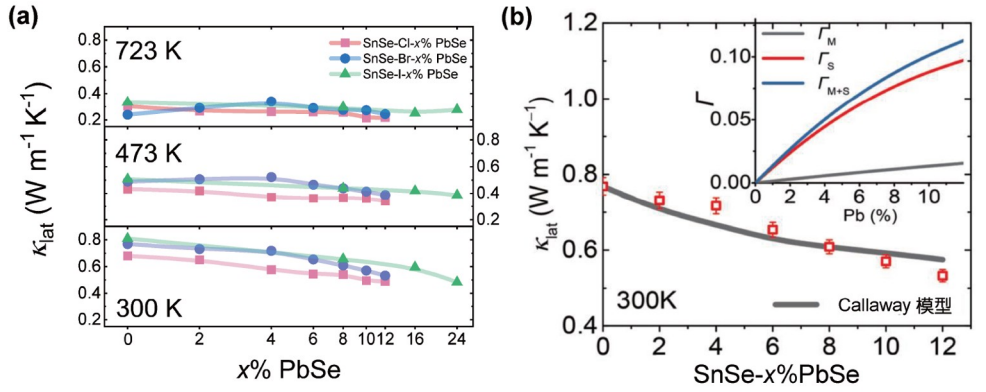


图 5 (网络版彩色)卤素掺杂与PbSe固溶对n型SnSe晶体面外方向的晶格热导率κ_{lat}的影响. (a) 300、473、723 K下, PbSe固溶的卤素掺杂n型SnSe晶体的κ_{lat}随温度T的演化[26,29,31,34]; (b) 300 K下PbSe固溶的Br掺杂n型SnSe晶体的κ_{lat}及Callaway模型模拟, 插图为PbSe固溶引起的应力与质量波动对κ_{lat}的影响[31], Copyright © 2019, Wiley-VCH Verlag GmbH & Co. KGaA, Weinheim

Figure 5 (Color online) Effect of halogen doping and PbSe alloying on the lattice thermal conductivity κ_{lat} of n-type SnSe crystals along the out-of-plane direction. (a) κ_{lat} as a function of temperature T for PbSe alloying halogen-doped n-type SnSe crystals at 300, 473, and 723 K[26,29,31,34]. (b) κ_{lat} of PbSe alloying Br-doped n-type SnSe crystals at 300 K and Callaway model simulations. The inset shows the effect of stress and mass fluctuations on κ_{lat} due to PbSe alloying[31], Copyright © 2019, Wiley-VCH Verlag GmbH & Co. KGaA, Weinheim

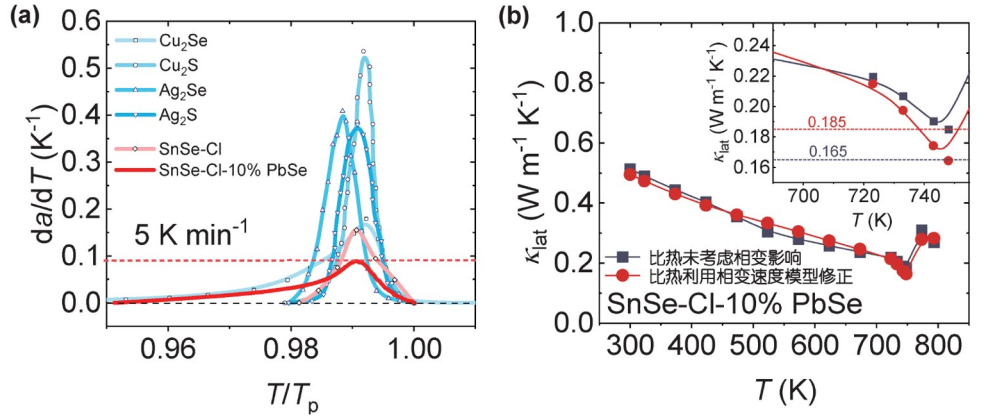


图 6 (网络版彩色)(a) 不同相变材料的相变速度[26,40,41]; (b) 相变对n型SnSe晶体面外方向晶格热导率的影响[26]

Figure 6 (Color online) (a) Phase transition rates for different phase transition materials[26,40,41]; (b) effect of phase transition on lattice thermal conductivity of n-type SnSe crystals along the out-of-plane direction[26]

响, 经相变速度模型修正后, SnSe-Cl-10%PbSe在748 K获得了~0.18 W m^{-1} K^{-1}的超低κ_{lat}, 证实了*Pnma*相的SnSe在面外方向的超低晶格热导率优势.

3 总结与展望

SnSe独特的各向异性层状结构及相变过程赋予了p型与n型SnSe晶体优异的热电性能, 使SnSe成为潜在的下一代商用热电材料之一. 当前, 可实现SnSe全温区高效n型掺杂的施主杂质主要为Cl、Br、I等卤素元素; 3种施主杂质掺杂的n型SnSe晶体的热电输运特性排序如下: ① n: SnSe-Br > SnSe-Cl > SnSe-I; ② μ: SnSe-Cl > SnSe-I > SnSe-Br; ③ m^*: SnSe-Cl ≈ SnSe-Br > SnSe-I; ④ Ξ: SnSe-Cl < SnSe-Br ≈ SnSe-I; ⑤ κ_{lat}: SnSe-Cl < SnSe-Br ≈ SnSe-I. 综合来看, SnSe-Cl在中低温区具有性能优势, SnSe-Br凭借较大的n优势在高温区具有性能优势. 固溶PbSe是优化n型SnSe热电性能的有效手段, 其可通过促进能带简并与增大r实现对n型SnSe晶体面外电输运性能的优化; 固溶PbSe会降低面内方向的r, 因此对面内热电性能的优化效果不及面外方向. SnSe由*Pnma*相到*Cmcm*相的临界相变速度较低, 其临界相变对热导率的影响小于Ag_2S、Cu_2Se等热电相变材料; 经相变速度模型修正的n型SnSe晶体面外方向κ_{lat}为~0.18 W m^{-1} K^{-1}, 证实了SnSe在*Pnma*相的面外超低晶格热导率优势.

构建高性能热电器件需要性能相匹配的高性能p型与n型热电材料. 材料性能方面, n型SnSe晶体与p型SnSe晶体仍有一定差距, 大幅提升n型SnSe晶体的近室温热电性能、优化其宽温域热电性能是n型SnSe晶体当前面临的主要挑战; 相比于面外方向, n型SnSe晶体面内方向在近室温区域拥有电输运性能的显著优势, 两方向近室温热电性能差异不大; 因此, 优化n型SnSe晶体面内性能可能是实现近室温全SnSe基热电制冷技术的关键. 器件装配方面, n型SnSe晶体目前在该领域远落后于p型SnSe晶体, 其原因主要在于缺乏适配于n型SnSe的接触层材料, 以及SnSe面外方向较低的机械性能; 开发n型SnSe晶体面内性能虽能避免SnSe面外较弱机械性能为制备热电器件带来的挑战, 但仍需面对缺乏合适接触材料的困难; 因此, 开发适合于n型SnSe晶体的低界面电阻接触材料是n型SnSe晶体未来能否进一步发展的关键.

参考文献

1 Mao J, Chen G, Ren Z. Thermoelectric cooling materials. Nat Mater, 2021, 20: 454–461
2 Shi X L, Zou J, Chen Z G. Advanced thermoelectric design: From materials and structures to devices. Chem Rev, 2020, 120: 7399–7515
3 Yuan J, Li M, Wang H. Intrinsically ultralow lattice thermal conductivity and giant thermoelectric effect in Ag-based intercalated layered crystalline solids. Phys Rev B, 2024, 109: 235202
4 Ying P, Villoro R B, Bahrami A, et al. Performance degradation and protective effects of atomic layer deposition for Mg-based thermoelectric modules. Adv Funct Mater, 2024, 2406473
5 Chen C, Wang T, Yu Z, et al. Modulation doping enables ultrahigh power factor and thermoelectric ZT in n-type $Bi_2Te_{2.7}Se_{0.3}$. Adv Sci, 2022, 9: 2201353
6 Wang S J, Panhans M, Lashkov I, et al. Highly efficient modulation doping: A path toward superior organic thermoelectric devices. Sci Adv, 2022, 8: eabl9264
7 Zheng Z H, Shi X L, Ao D W, et al. Rational band engineering and structural manipulations inducing high thermoelectric performance in n-type $CoSb_3$ thin films. Nano Energy, 2021, 81: 105683
8 Xiao Y, Wang D, Zhang Y, et al. Band sharpening and band alignment enable high quality factor to enhance thermoelectric performance in n-type PbS. J Am Chem Soc, 2020, 142: 4051–4060
9 Pei Y, Wang H, Snyder G J. Band engineering of thermoelectric materials. Adv Mater, 2012, 24: 6125–6135
10 Qin B, Wang D, Hong T, et al. High thermoelectric efficiency realized in SnSe crystals via structural modulation. Nat Commun, 2023, 14: 1366
11 Dutta M, Pal K, Etter M, et al. Emphanisis in cubic $(SnSe)_{0.5}(AgSbSe_2)_{0.5}$: Dynamical off-centering of anion leads to low thermal conductivity and high thermoelectric performance. J Am Chem Soc, 2021, 143: 16839–16848
12 Qin Y, Qin B, Hong T, et al. Grid-plainification enables medium-temperature PbSe thermoelectrics to cool better than Bi_2Te_3. Science, 2024, 383: 1204–1209
13 Hu C, Xia K, Fu C, et al. Carrier grain boundary scattering in thermoelectric materials. Energy Environ Sci, 2022, 15: 1406–1422
14 Pei Y, Tan G, Feng D, et al. Integrating band structure engineering with all-scale hierarchical structuring for high thermoelectric performance in PbTe system. Adv Energy Mater, 2016, 7: 1601450
15 Qin B, Wang D, Zhao L. Slowing down the heat in thermoelectrics. InfoMat, 2021, 3: 755–789
16 Wang S, Zhang L, Hong T, et al. Realizing remarkable improvement of electrical performance in N-type $BiSbSe_3$ via *in situ* compositing. Adv Funct Mater, 2024, 34: 2310335
17 Li Z, Wang L, Abbas A, et al. Vacancy suppression and resonant level rendering extraordinary power factor in $Sn_{0.99}In_{0.01}Te$/tourmaline composite. Small, 2024, doi: 10.1002/smll.202402651: 2402651
18 Zhou Z, Huang Y, Wei B, et al. Compositing effects for high thermoelectric performance of Cu_2Se-based materials. Nat Commun, 2023, 14: 2410
19 Wang N, Li M, Xiao H, et al. Layered LaCuOSe: A promising anisotropic thermoelectric material. Phys Rev Appl, 2020, 13: 024038
20 Wang D, Huang Z, Zhang Y, et al. Extremely low thermal conductivity from bismuth selenohalides with 1D soft crystal structure. Sci China Mater, 2020, 63: 1759–1768
21 Pandey T, Nissimagoudar A S, Mishra A, et al. Ultralow thermal conductivity and high thermoelectric figure of merit in mixed valence In_5X_5Br (X = S, and Se) compounds. J Mater Chem A, 2020, 8: 13812–13819
22 Zhao L. SnSe/SnS: Multifunctions beyond thermoelectricity. MatLab, 2022, 1: 1–20
23 Zhao L D, Lo S H, Zhang Y, et al. Ultralow thermal conductivity and high thermoelectric figure of merit in SnSe crystals. Nature, 2014, 508: 373–377

24 Zhou Z, Zhou X. Realizing ultrahigh average figure of merit through manipulating layered phonon-electron decoupling. Sci China Mater, 2022, 65: 1987–1988

25 Liu D, Wang D, Hong T, et al. Lattice plainification advances highly effective SnSe crystalline thermoelectrics. Science, 2023, 380: 841–846

26 Su L, Wang D, Wang S, et al. High thermoelectric performance realized through manipulating layered phonon-electron decoupling. Science, 2022, 375: 1385–1389

27 Lee Y K, Ahn K, Cha J, et al. Enhancing p-type thermoelectric performances of polycrystalline SnSe via tuning phase transition temperature. J Am Chem Soc, 2017, 139: 10887–10896

28 Dewandre A, Hellman O, Bhattacharya S, et al. Two-step phase transition in SnSe and the origins of its high power factor from first principles. Phys Rev Lett, 2016, 117: 276601

29 Chang C, Wu M, He D, et al. 3D charge and 2D phonon transports leading to high out-of-plane *ZT* in n-type SnSe crystals. Science, 2018, 360: 778–783

30 Qin B, Wang D, He W, et al. Realizing high thermoelectric performance in p-Type SnSe through crystal structure modification. J Am Chem Soc, 2019, 141: 1141–1149

31 Chang C, Wang D, He D, et al. Realizing high-ranged out-of-plane ZTs in N-type SnSe crystals through promoting continuous phase transition. Adv Energy Mater, 2019, 9: 1901334

32 Yang J, Zhang G, Yang G, et al. Outstanding thermoelectric performances for both p- and n-type SnSe from first-principles study. J Alloys Compd, 2015, 644: 615–620

33 Duong A T, Nguyen V Q, Duvjir G, et al. Achieving ZT=2.2 with Bi-doped n-type SnSe single crystals. Nat Commun, 2016, 7: 13713

34 Su L, Shi H, Wang S, et al. Enhancing carrier mobility and Seebeck coefficient by modifying scattering factor. Adv Energy Mater, 2023, 13: 2300312

35 Shi H, Su L, Bai S, et al. Realizing high in-plane carrier mobility in n-type SnSe crystals through deformation potential modification. Energy Environ Sci, 2023, 16: 3128–3136

36 Mao L, Yin Y, Zhang Q, et al. Fermi-surface dynamics and high thermoelectric performance along the out-of-plane direction in n-type SnSe crystals. Energy Environ Sci, 2020, 13: 616–621

37 Zhou Y, Li W, Wu M, et al. Influence of defects on the thermoelectricity in SnSe: A comprehensive theoretical study. Phys Rev B, 2018, 97: 245202

38 Sheng Z, Guo C, Hu S, et al. Routes to high-carrier-density doping in thermoelectric SnSe. J Phys Chem C, 2022, 126: 1230–1241

39 Agne M T, Voorhees P W, Snyder G J. Phase transformation contributions to heat capacity and impact on thermal diffusivity, thermal conductivity, and thermoelectric performance. Adv Mater, 2019, 31: e1902980

40 Chen H, Yue Z, Ren D, et al. Thermal conductivity during phase transitions. Adv Mater, 2019, 31: e1806518

41 Zhou C, Lee Y K, Yu Y, et al. Polycrystalline SnSe with a thermoelectric figure of merit greater than the single crystal. Nat Mater, 2021, 20: 1378–1384

Summary for “n型硒化锡晶体热电材料研究进展”

Recent progress in n-type SnSe crystals thermoelectric materials

Lizhong Su* & Xiaokun Feng

School of Materials Science and Engineering, Taiyuan University of Science and Technology, Taiyuan 030024, China
* Corresponding author, E-mail: sulizhong@tyust.edu.cn

Thermoelectric energy conversion technology can directly convert thermal and electrical energy to each other based on thermoelectric devices, and has a huge potential in power generation and thermoelectric cooling. The energy conversion efficiency of thermoelectric devices is determined by the average dimensionless figure of merit (ZT_{ave}) of the thermoelectric material in a certain temperature range. Manufacturing high-performance thermoelectric devices requires both high-performance p- and n-type thermoelectric materials with matching properties. Tin selenide (SnSe) is an intrinsic p-type wide-bandgap thermoelectric material. The anisotropic layered structure and unique phase transition of SnSe endow both p- and n-type SnSe crystals with excellent thermoelectric properties. Thus, SnSe crystals have attracted much attention in the thermoelectric field and are considered as one of the potential next-generation commercial thermoelectric materials. Currently, p-type SnSe crystals achieve a ZT_{ave} of ~2.2 between 300–773 K and a ZT of ~1.5 at 300 K. However, n-type SnSe crystals can only achieve a ZT_{ave} of 1.7 between 300–773 K and a ZT of ~0.5 at 300 K. Apparently, the thermoelectric performance of n-type SnSe crystals is still dissatisfactory compared to p-type SnSe crystals, especially for near room temperature. Optimizing the thermoelectric properties of n-type SnSe crystals has become the priority for the realization of all SnSe-based thermoelectric devices. Therefore, it is indispensable to summarize the research progress in n-type SnSe crystals and to develop a comprehensive understanding of their thermoelectric transport properties.

In this review, we first summarized the recent progress in n-type SnSe crystals thermoelectric materials and analyzed the similarities and differences in the thermoelectric transport properties of n-type SnSe crystals doped with different donor impurities (bismuth, chlorine, bromine, and iodine). In general, halogen-doped SnSe crystals possess “two-dimensional phonon and three-dimensional charge” thermoelectric transport and show higher performance along the out-of-plane direction. Chlorine-doped SnSe crystals have a performance advantage in the near room and medium temperature regions resulting from the higher carrier mobility, and bromine-doped SnSe crystals show superior performance at high temperatures due to their relatively larger carrier concentration. Differently, bismuth-doped SnSe crystals show higher performance along the in-plane direction than the out-of-plane direction, and possess the highest thermoelectric performance along the in-plane direction compared to halogen-doped SnSe crystals due to their largest carrier concentration at high temperatures. Secondly, we compared the differences between the electrical properties of n-type SnSe crystals along the in-plane and out-of-plane directions due to the enhanced anisotropic carrier scattering factor induced by alloying lead selenide. Alloying lead selenide increases the scatter factor along the out-of-plane direction but decreases the scatter factor along the in-plane direction, which enlarges the Seebeck coefficient difference between the out-of-plane direction and the in-plane direction. Finally, we described the effect of SnSe phase transition on its thermal conductivity. The effect of the phase transition of SnSe on thermal conductivity mainly comes from the critical phase transition from *Pnma* to *Cmcm* phase; the continuous phase transition has little effect on thermal conductivity. We also discussed the upcoming research priorities and challenges for n-type SnSe crystals thermoelectric materials. This review describes the progress in n-type SnSe crystal thermoelectric materials, which helps researchers gain a comprehensive understanding of the thermoelectric transport of n-type SnSe crystals, and points out the direction for the future development of n-type SnSe crystals.

thermoelectric materials, crystals, layered structure, phase transition materials, n-type tin selenide

doi: 10.1360/TB-2024-0796